



HAL
open science

Phase diagram of polyelectrolyte solutions

K. Kaji, H. Urakawa, T. Kanaya, R. Kitamaru

► **To cite this version:**

K. Kaji, H. Urakawa, T. Kanaya, R. Kitamaru. Phase diagram of polyelectrolyte solutions. *Journal de Physique*, 1988, 49 (6), pp.993-1000. 10.1051/jphys:01988004906099300 . jpa-00210788

HAL Id: jpa-00210788

<https://hal.science/jpa-00210788>

Submitted on 4 Feb 2008

HAL is a multi-disciplinary open access archive for the deposit and dissemination of scientific research documents, whether they are published or not. The documents may come from teaching and research institutions in France or abroad, or from public or private research centers.

L'archive ouverte pluridisciplinaire **HAL**, est destinée au dépôt et à la diffusion de documents scientifiques de niveau recherche, publiés ou non, émanant des établissements d'enseignement et de recherche français ou étrangers, des laboratoires publics ou privés.

Classification
Physics Abstracts
61.25 — 61.40K

Phase diagram of polyelectrolyte solutions

K. Kaji, H. Urakawa, T. Kanaya and R. Kitamaru

Institute for Chemical Research, Kyoto University, Uji, Kyoto-fu 611, Japan

(Reçu le 25 juin 1987, accepté le 25 septembre 1987)

Résumé. — On construit le diagramme de phases des solutions de polyélectrolytes vinyliques en fonction de leur degré de polymérisation et de leur concentration sur la base des théories de de Gennes *et al.* et d'Odijk et aussi de la longueur de persistance calculée par Le Bret. On différencie d'abord les régions diluée et semidiluée de ces solutions. On sépare ensuite la région semidiluée en trois régimes, qui sont, par ordre de concentration décroissante, les régimes isotrope, de transition et de réseau. On sépare aussi la région diluée en deux régimes, l'un ordonné et l'autre désordonné. Les régimes isotrope et de réseau ont été décrits par de Gennes, et le régime de transition par Odijk. Les régimes ordonné et désordonné peuvent être distingués selon l'existence de corrélations causées par les répulsions électrostatiques. On utilise la diffusion des rayons X aux petits angles pour confirmer la concentration du passage dilué-semidilué dans des solutions de poly(styrène sulfonate) de sodium. D'autre part, une analyse préliminaire de la distribution des distances confirme la concentration de fusion C_m^* entre les régimes isotrope et de transition. A présent nous n'avons pas d'information sur le passage entre les régimes de réseau et de transition, ni sur le passage ordonné-désordonné.

Abstract. — The phase diagram of vinyl polyelectrolyte solutions with the degree of polymerization and the concentration is constructed, based on the theories of de Gennes *et al.* and Odijk, and the electrostatic persistence length calculated by Le Bret. The polyelectrolyte solutions are differentiated between the dilute and semidilute regions. The semidilute region is separated into three regimes, called isotropic, transition, and lattice in the order of decreasing concentration, while the dilute region is divided into two regimes, termed order and disorder. The isotropic and lattice regimes are depicted by de Gennes *et al.*, and the transition regime is described by Odijk. The order and disorder regimes are distinguished from each other by whether an intermolecular single correlation due to electrostatic repulsive forces exists or not. The dilute-semidilute crossover concentration has been confirmed in a concentration range between 0.01 and 1.0 mol/l from the small-angle X-ray scattering of sodium poly(styrene sulfonate) (NaPSS) solutions. The melting crossover C_m^* between isotropic and transition regimes is supported by some preliminary results of distance distribution analysis. Until now we have no information on the lattice-transition crossover and the order-disorder crossover.

1. Introduction.

In the previous paper [1], we studied the structure of semidilute polyelectrolyte solutions without added salts by means of small angle X-ray scattering (SAXS), and confirmed that in a higher concentration (0.2 monomer mol/l) the isotropic model proposed by de Gennes *et al.* [2] is valid. However, the theoretical approaches by de Gennes *et al.* [2] and Odijk [3] suggest that the polyelectrolyte solutions assume different structures depending on the concentration and the contour length or degree of polymerization. In this study we therefore construct the phase diagram with the degree of polymerization

and the concentration for vinyl polyelectrolyte aqueous solutions at ambient temperature (see Fig. 1) based on the above two theoretical approaches and the electrostatic persistence lengths, calculated theoretically by Le Bret [4] and confirmed experimentally by Nierlich *et al.* [5]. During the construction of the phase diagram the review of Mandel [6] was also very suggestive.

As the phase diagram is undoubtedly of great importance in any static or dynamic study on polyelectrolyte solutions, it should be confirmed experimentally. We therefore have tried to confirm

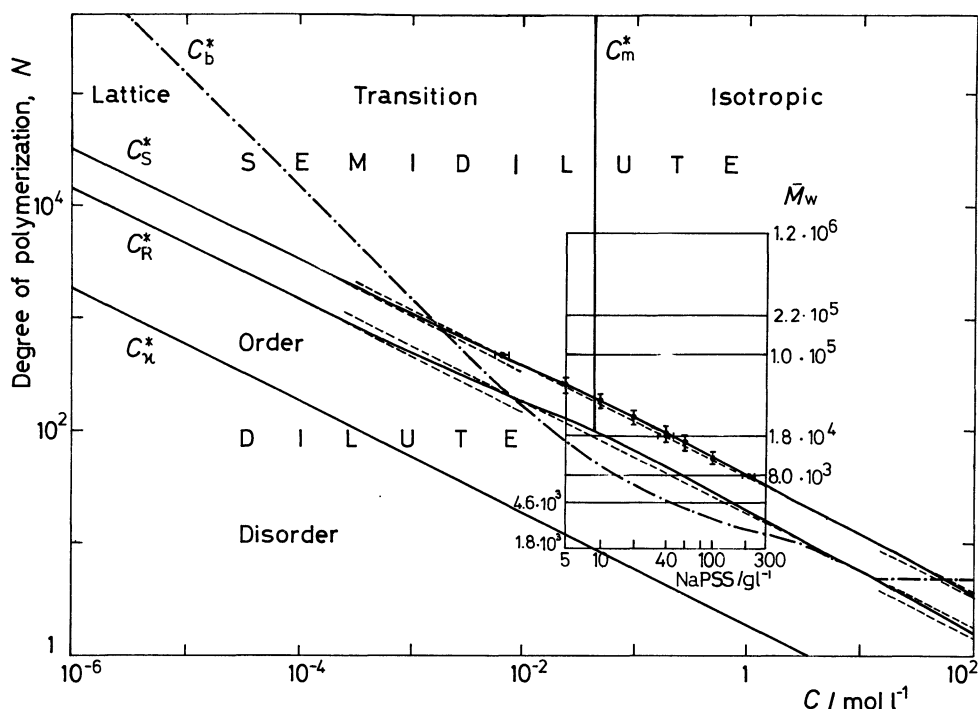


Fig. 1. — Phase diagram for vinyl polyelectrolyte solutions with the degree of polymerization N and the concentration C at ambient temperature. The crossover lines and regimes are explained in the text. The area enclosed within a square is the region where the SAXS experiments were carried out for NaPSS solutions.

this phase diagram by using the SAXS technique. For this purpose the theoretical studies by Koyama [7] are useful which provide the relationships between the maximum position of the scattering intensity and the polymer concentration in the dilute and semidilute regions.

2. Phase diagram.

To describe the size of polyions we employ the wormlike-chain model and assume that the total persistence length b_t can be given by the sum of electrostatic b_e and intrinsic b_0 components :

$$b_t = b_e + b_0. \quad (1)$$

As Nierlich *et al.* [5] estimated $b_0 = 12 \text{ \AA}$, it may be neglected unless the concentration C is very high. According to Le Bret [4], b_e is inversely proportional to C in the concentration range below about 10^{-2} mol/l , and is nearly proportional to $C^{-1/2}$ in the range between ca. 0.1 and 3 mol/l, which is also predicted by de Gennes *et al.* [8]. Based on these results for b_e , it can be assumed that the polyion at the dilute-semidilute crossover concentration behaves approximately as a rodlike chain or a chain with b_e being equal to the contour length l depending on whether the concentration is below or above a critical value of about $1 \times 10^{-3} \text{ mol/l}$, respectively.

As the polyion size may be given by the mean-square end-to-end distance [9]

$$\langle R^2 \rangle = 2 b_t^2 (\alpha - 1 + e^{-\alpha}) \quad (2)$$

where $\alpha = l/b_t$, the dilute-semidilute crossover concentration for this size becomes

$$C_R^* = \frac{N}{(4/3) \pi (\langle R^2 \rangle^{1/2} / 2)^3} = \begin{cases} 2.03 \times 10^2 N^{-2} \text{ (mol/l)} & \text{for } \alpha = 0 \\ 3.22 \times 10^2 N^{-2} \text{ (mol/l)} & \text{for } \alpha = 1. \end{cases} \quad (3)$$

Here N is the degree of polymerization, and the length a of a monomeric unit is taken to be 2.5 \AA in $l = aN$ since we are considering vinyl polyelectrolytes.

However, scattering techniques such as X-ray, neutron, and light scattering do not feel the crossover for $\langle R^2 \rangle$, but detect that for radius of gyration, which is given by [9] :

$$\langle S^2 \rangle = b_t^2 \left[\frac{\alpha}{3} - 1 + \frac{2}{\alpha^2} (\alpha - 1 + e^{-\alpha}) \right]. \quad (4)$$

The crossover concentration for $\langle S^2 \rangle$ becomes

$$C_S^* = \frac{N}{(4/3) \pi \langle S^2 \rangle^{3/2}} = \begin{cases} 1.05 \times 10^3 N^{-2} \text{ (mol/l)} & \text{for } \alpha = 0 \\ 1.40 \times 10^3 N^{-2} \text{ (mol/l)} & \text{for } \alpha = 1. \end{cases} \quad (5)$$

From equations (3) and (4) we can draw the dilute-semidilute crossovers for $\langle R^2 \rangle$ and $\langle S^2 \rangle$ in the phase diagram as shown in figure 1. The exact crossovers calculated from b_t given by Le Bret are designated by solid curves, while the approximate ones of equations (3) and (5) are indicated by broken lines.

Based on the theories by de Gennes *et al.* [2] and Odijk [3], the semidilute region may be further separated into at least three regimes, called lattice, transition, and isotropic. The lattice and isotropic regimes are depicted by de Gennes and the transition regime is described by Odijk. The crossover C_b^* between the lattice and the transition regime is obtained as a concentration at $b_t \simeq l$. The concentration ranges which satisfy the condition $b_t \simeq l$ in the semidilute region are below 0.8×10^{-2} mol/l and above 10 mol/l. The crossover for these two ranges are

$$C_b^* = 1.48 N^{-1} \text{ (mol/l)} \quad \text{for } C < 0.8 \times 10^{-2} \text{ (mol/l)} \quad (6)$$

and

$$N = 4.8 \quad \text{for } C > 15 \text{ (mol/l)} \quad (b_e = 0). \quad (7)$$

Therefore, the lattice structure could be found in two separate regions: very dilute-high N region and very concentrated-low N region. The latter lattice region has not been so far predicted. The curve C_b^* in a concentration range between 0.8×10^{-2} and 10 mol/l is not related to any crossover because it is in the dilute region. The crossover between the transition and the isotropic regime is a concentration C_m^* where the lattice melts completely. Based on the concept of de Gennes [2], Odijk [3] calculated this concentration

$$C_m^* \simeq \frac{0.04}{4 \pi Q^2 a} = 4.32 \times 10^{-2} \text{ (mol/l)}. \quad (8)$$

Here $Q = e^2 / (\epsilon k_B T)$ is the Bjerrum length, and e , ϵ and $k_B T$ are the elementary charge, the dielectric constant of the solvent, and the Boltzmann factor, respectively. Mandel [6] discussed another crossover C_ξ^* at $b_c \sim \xi$ (correlation length) in the transition regime. However, it might be considered unnecessary because the b_t of Le Bret leads to $C_\xi^* = 3.5 \times 10^{-2}$ mol/l, which almost agrees to C_m^* .

The dilute region may be also distinguished into two regimes, termed order and disorder. The former is the region where intermolecular electrostatic correlation exists and will provide a correlation peak in the scattering intensity. On the other hand, the latter is the region where the intermolecular distance is too far for electrostatic interactions to work among polyions and will not show a clear scattering peak. The crossover between these two regimes, C_κ^* , can be estimated as a concentration where the electro-

static screening length κ^{-1} is equal to half a distance between two neighbouring polyion centres. In the case of vinyl polyelectrolytes the electrostatic screening length is given by Odijk [3] to be

$$\kappa^{-1} = (4 \pi a C)^{-1/2}. \quad (9)$$

If the centres of polyions are arranged on a body-centred cubic lattice with edge D ,

$$D = (2 N / C)^{1/3} \quad (10)$$

as de Gennes *et al.* showed. Combining equations (9) and (10) by $\kappa^{-1} = D/2$, we obtain

$$C_\kappa^* = \frac{1}{4 \pi^3 a^3 N^2} = 3.43 N^{-2} \text{ (mol/l)}. \quad (11)$$

3. Experimental.

3.1 SAMPLE. — Sodium poly(styrene sulfonate) (NaPSS) samples for GPC standards of Pressure Chemical Co. were used: the weight-average molecular weights \bar{M}_w of these samples are 1.8×10^3 , 4.6×10^3 , 8.0×10^3 , 1.8×10^4 , 1.0×10^5 , 2.2×10^5 , and 1.2×10^6 . Their polydispersity, characterized by the ratio \bar{M}_w / \bar{M}_n where \bar{M}_n is the number-average molecular weight, is 1.10 except for the sample with $\bar{M}_w = 1.8 \times 10^3$ and $\bar{M}_w / \bar{M}_n = 1.2$. Sample purification was carried out by deionizing with ion-exchange resins Amberlite IR-120B and IRA-400 of Organo Co., neutralizing with sodium hydroxide, and then lyophilizing. The purified samples after freeze-drying were kept in a desiccator until use. The total concentration of the aqueous solution of NaPSS was changed between 5 and 200 g/l or between 0.024 and 0.97 mol/l for each sample.

3.2 SAXS MEASUREMENTS. — The SAXS intensity measurements were carried out by using a Kratky compact camera with a proportional counter and Ni-filtered pulse-height-analysed $\text{CuK}\alpha$ radiation generated at 40 kV and 45 mA. From the observed intensity of the sample solution corrected for absorption the scattering intensity of water was subtracted. Then, the slit correction for the length and width of the beam was made by a method developed in our laboratory [10], which has an advantage that the observed curve is desmeared reasonably and unequivocally. The further details were described previously [1].

4. Experimental results.

The observed SAXS curves after correction are shown in figures 2 and 3 as examples for concentration and degree-of-polymerization dependences, respectively. The intensity is normalized per monomer unit; the observed intensity $I(q)$ is divided by the concentration C , i.e., $I(q)/C$. q is the magnitude of

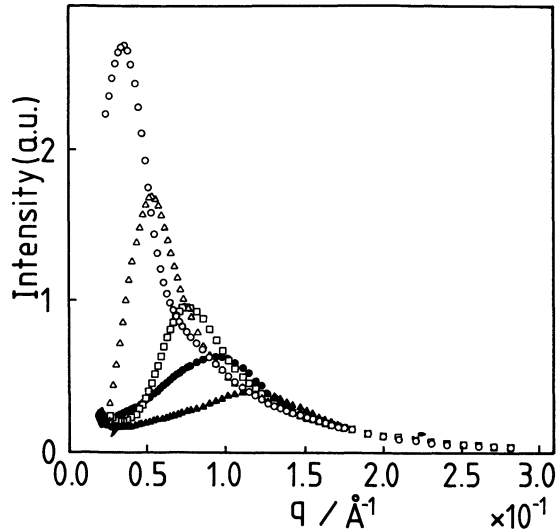


Fig. 2. — The concentration dependence of SAXS intensity curves for NaPSS when $\bar{M}_w = 1.0 \times 10^5$. The concentrations are $C = 10$ g/l (○), 20 g/l (△), 40 g/l (□), 60 g/l (●) and 100 g/l (▲).

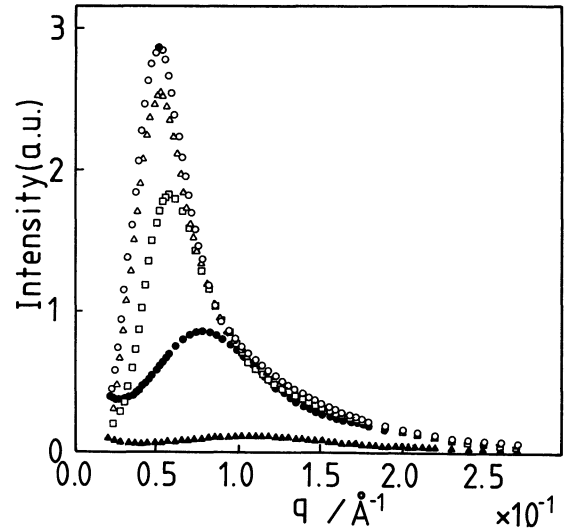


Fig. 3. — The molecular-weight dependence of SAXS intensity curves for NaPSS when $C = 20$ g/l. The molecular weights are $\bar{M}_w = 1.2 \times 10^6$ (○), 1.0×10^5 (△), 1.8×10^4 (□), 4.6×10^3 (●) and 1.8×10^3 (▲).

scattering vector : $q = 4 \pi \sin \theta / \lambda$ where θ is a Bragg angle and λ is a wavelength of X-ray (CuK α). Figure 2 shows that the peak position q_m increases and the intensity at q_m decreases with increasing C . This means that the correlation length ξ and the correlation strength decreases with increasing C as a natural result. As seen from figure 3, the intensity at q_m increases with degree of polymerization N when the concentration is constant, which means that the higher N , the stronger the correlation because the electrostatic repulsion forces become stronger. The

q_m decreases with increasing N , but above a critical value of N it remains constant. This critical value N^* is considered a dilute-semidilute crossover point as will be described later (see Fig. 7). All the observed values of q_m 's are summarized in table I. Exactly speaking, the observed q_m 's should be corrected for the cross-sectional size of a polyion, but such a correction is very small (less than 1%), and practically unnecessary. The radius of the cross-section, r_0 , used for this correction was determined experimentally by using the same method as previ-

Table I. — Observed q_m 's for NaPSS aqueous solutions (*).

C		$q_m / \text{Å}^{-1}$						
g/l	mol/l	$\bar{M}_w = 1.8 \times 10^3$	4.6×10^3	8.0×10^3	1.8×10^4	1.0×10^5	2.2×10^5	1.2×10^6
5	0.024	—	0.0516	0.0463	0.0346	0.0230	0.0223	0.0241
10	0.049	0.0863	0.0642	0.0589	0.0438	0.0362	0.0353	0.0312
20	0.097	0.1080	0.0779	0.0743	0.0588	0.0528	0.0510	0.0515
40	0.190	0.1270	0.0977	0.0924	—	0.0765	—	0.0752
41	0.200	—	—	—	0.813	—	—	—
42	0.210	—	—	—	—	—	0.0768	—
60	0.290	0.1380	0.1090	0.1060	—	0.0948	—	0.0916
62	0.300	—	—	—	0.0957	—	—	—
63	0.310	—	—	—	—	—	0.0937	—
73	0.360	—	—	—	—	—	0.0979	—
100	0.490	0.1540	0.1270	0.1250	0.1240	0.1170	—	0.1140
200	0.970	0.1790	—	0.1600	0.1660	0.1590	—	0.1730
300	1.500	—	—	—	—	0.1860	—	—

(*) The polydispersity \bar{M}_w / \bar{M}_n is 1.10 except for $\bar{M}_w = 1.8 \times 10^4$ with $\bar{M}_w / \bar{M}_n = 1.20$.

ously reported [1]; $r_0 = 8.3 \pm 0.3 \text{ \AA}$ was obtained as the average value for various concentrations and degrees of polymerization.

The concentration dependence of the peak intensity per monomer unit, $I(q_m)/C$, is shown for several molecular weights \bar{M}_w in figure 4. The variation of the peak intensity, which was qualitatively described above, is seen quantitatively in this figure. When the concentration is above ca. 200 g/l, no molecular weight dependence is seen, but below 200 g/l it increases with decreasing concentration. When \bar{M}_w is larger than about 1×10^5 , the intensity does not come to depend on \bar{M}_w . In this case the intensity variation seems to obey the relationship $I(q_m)/C \sim C^{-1/2}$ for concentrations below 20 g/l, as Jannink reviewed [16] and Koyama predicted theoretically [7]. Above 20 g/l, the intensity however decreases more rapidly than the above relation, which is not as yet explained.

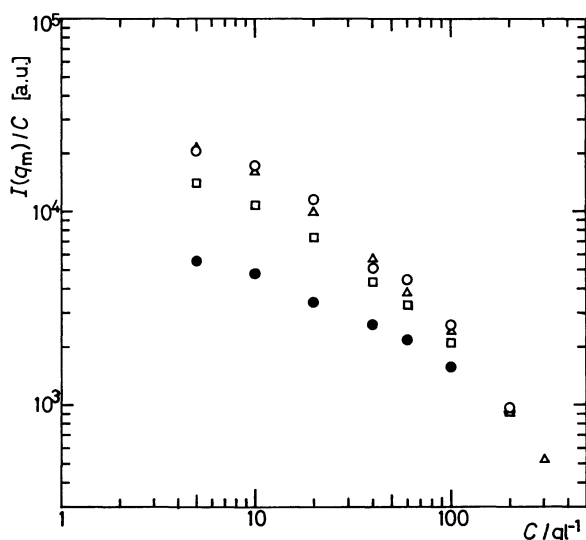


Fig. 4. — The concentration dependence of the peak intensity per monomer unit, $I(q_m)/C$. The molecular weights are $\bar{M}_w = 1.2 \times 10^6$ (○), 1.0×10^5 (△), 1.8×10^4 (□) and 4.6×10^3 (●).

5. Determination of dilute-semidilute crossover by SAXS.

The dilute-semidilute crossover for radius of gyration C_s^* in the phase diagram of figure 1 can be confirmed by small-angle X-ray scattering measurements. In the case of salt-free solutions of the usual concentrations a single intensity peak is observed in the small angle X-ray or neutron scattering [1, 11]. The maximum position of this peak q_m is related to the concentration C [2, 7, 12]; $q_m \sim C^{1/2}$ for semidilute solutions, and $q_m \sim C^{1/3}$ for the dilute solutions.

Therefore we can detect C_s^* from the intersection point of these two relations in $\log q_m - \log C$ plot. Although the theory of Koyama [7] predicts that this crossover is not sharp and the exponent n of $q_m \sim C^n$ in the dilute solutions as well as its coefficient gradually changes with C and N , the experimental results show that for polymers with N not less than about 40 the exponent $n = 1/3$ practically remains constant independent of C and N except near the crossover point. We therefore estimate crossover concentrations for polymers with $\bar{N} > 40$ or $\bar{M}_w > 8 \times 10^3$.

To estimate the crossovers three different plots have been carried out: (1) $q_m - C$ (2) $q_m - C/N$, and (3) $q_m - N$, respectively in figures 5-7. Figure 5 shows that q_m increases with C as $q_m \sim C^{1/3}$ when C and N are not high, but above a critical concentration it obeys the equation

$$q_m = 1.7 C^{1/2} \quad (12)$$

where q_m and C are given in \AA^{-1} and mol/l, respectively. The equation (12) agrees well to the theoretical equation derived by Koyama [7]

$$q_m = 1.78 C^{1/2}, \quad (13)$$

which corresponds to $q_m = 7.24 C^{1/2}$ where C is expressed in number of monomers per \AA^3 . This critical concentration corresponds to a dilute-semidilute crossover at higher concentrations. On the other hand, the $q_m - C/N$ plot in figure 6 provides the crossovers at lower concentrations. In this plot the relation in the dilute region can be expressed by

$$q_m = 0.54 (C/N)^{1/3} \quad (14)$$

which agrees almost to a relation between q_m and the

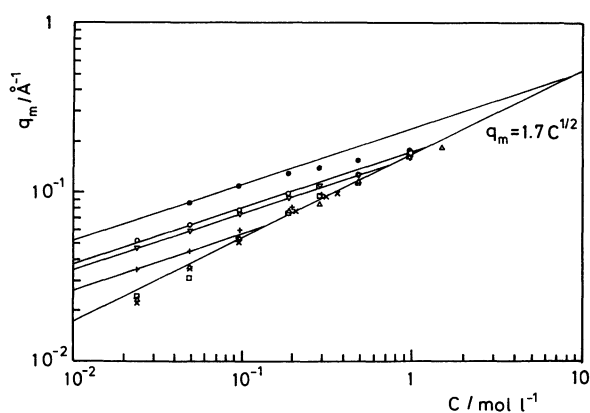


Fig. 5. — The $q_m - C$ plot in logarithmic scales for NaPSS solutions. $q_m = 1.7 C^{1/2}$ indicates the observed relation for semidilute solutions. $\bar{M}_w = 1.8 \times 10^3$ (●), 4.6×10^3 (○), 8.0×10^3 (▽), 1.8×10^4 (+), 1.0×10^5 (△), 2.2×10^5 (×) and 1.2×10^6 (□).

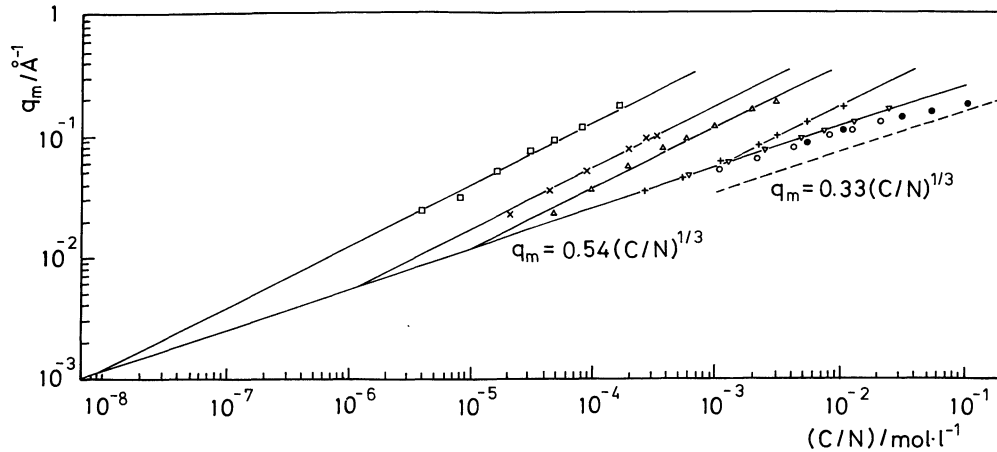


Fig. 6. — The $q_m - C/N$ plot in logarithmic scales for NaPSS solutions. $q_m = 0.54 (C/N)^{1/3}$ indicates the observed relation for dilute solutions. $q_m = 0.33 (C/N)^{1/3}$ is the relation for sufficiently dilute solutions given by Koyama [7]. See legends of figure 5 with regard to symbols.

average correlation length ξ_G between polyion centres derived from polymer concentration :

$$q_m = 2 \pi / \xi_G = 0.53 (C/N)^{1/3}. \quad (15)$$

However, when N is very small such as $N = 9$ and 22 , the observed q_m deviates from equation (14) as C increases. In a sufficiently dilute solution, polyions can be regarded as a point charge, i.e., the size of polyion is negligible. In a dilute near the semidilute region, however, q_m may be determined not only by the correlation length between polyion centres but also by the shape of polyion. In other words, q_m is affected by the form factor of a polyion. We expect that the deviation from $q_m = 0.54 (C/N)^{1/3}$ is due to the effect of the form factor of a polyion. The form factor can be obtained from the contour length and the persistence length, if we employ the wormlike-chain model. Therefore, the effects of the finite contour length on the electrostatic persistence length is essential to discuss the dependence of q_m on the molecular weight and the concentration. Weill *et al.* [17] have discussed this effects based on the theory of Odijk [18]. However, this problem is beyond the purpose of the present paper. We will discuss it elsewhere. As a reference the relation for sufficiently dilute solutions given by Koyama [7], $q_m = 0.33 (C/N)^{1/3}$, is also shown in figure 6.

The interpolation in the direction of N also provides the dilute-semidilute crossover because q_m depends on N in the dilute range, but it is independent of N in the semidilute range. As seen from figure 7, q_m is in fact constant in the semidilute range as predicted. However, in the dilute range the exponent of N does not agree to $-1/3$ as predicted from equation (14). The exponent decreases with increasing the concentration. This is due to the deviation of q_m for low N 's as described above. The

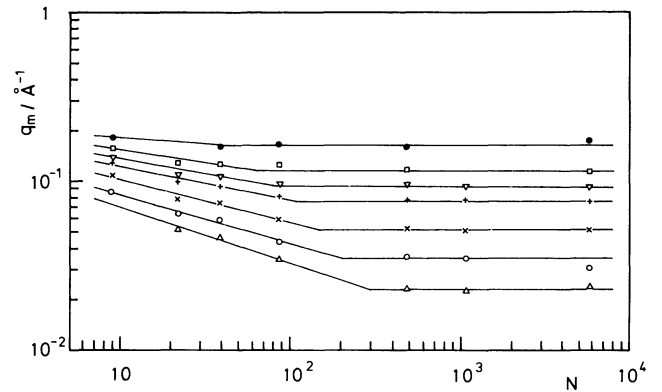


Fig. 7. — The $q_m - N$ plot in logarithmic scales for NaPSS solutions. $C = 200$ g/l (\bullet), 100 g/l (\square), 60 g/l (∇), 40 g/l ($+$), 20 g/l (\times), 10 g/l (\circ) and 5 g/l (Δ).

crossover degree-of-polymerization N^* was determined from the intersection point in figure 7. All the crossover values, the experimental errors of which are less than 10 %, determined from the above three plots are listed in tables II-IV.

The observed crossover concentrations C_3^* and degrees of polymerization N^* should be corrected for the polydispersity \bar{M}_w/\bar{M}_n of the sample. When the molecular weight distribution is approximated by the continuous Schulz-distribution function, the radius of gyration is expressed by the following [13]

$$\langle S^2 \rangle_U = \frac{l^2}{\alpha} \left\{ \frac{1}{3} \frac{1+2U}{1+U} - \frac{1}{\alpha} \left(1 - \frac{2}{\alpha} \right) - 2(1+U) \frac{1}{\alpha^3} \left[1 - \left(1 + \frac{U}{1+U} \alpha \right)^{-1/U} \right] \right\} \quad (16)$$

where $U = \bar{M}_w/\bar{M}_n - 1$ and $\alpha = l/b_t$. Within the observed concentration ranges α can be taken to be

Table II. — Dilute-semidilute crossover concentrations, C_S^* , determined from the $q_m - C$ plot. The values in parentheses are rough estimates.

\bar{M}_w	$C_S^*/\text{mol.l}^{-1}$	
	uncorrected	corrected for \bar{M}_w/\bar{M}_n
1.8×10^3	(8.0)	(14)
4.6×10^3	(1.2)	(1.6)
8.0×10^3	0.73	1.0
1.8×10^4	0.15	0.20

Table III. — Dilute-semidilute crossover concentrations, C_S^* , determined from the $q_m - C/N$ plot. The values in parentheses were obtained by extrapolating to very dilute concentrations where no experimental measurements were made.

\bar{M}_w	$C_S^*/\text{mol.l}^{-1}$	
	uncorrected	corrected for \bar{M}_w/\bar{M}_n
1.8×10^4	1.10×10^{-3}	1.5×10
1.0×10^5	4.37×10^{-3}	6.0×10^{-3}
2.2×10^5	(1.07×10^{-3})	(1.4×10^{-3})
1.2×10^6	(2.80×10^{-5})	(3.8×10^{-5})

Table IV. — Dilute-semidilute crossover degrees-of-polymerization, N^* , determined from the $q_m - N$ plot. The value in parentheses is a rough estimate.

C/gl^{-1}	N^*	
	uncorrected	corrected for \bar{M}_w/\bar{M}_n
5	3.0×10^2	2.6×10^2
10	2.1×10^2	1.8×10^2
20	1.5×10^2	1.3×10^2
40	1.1×10^2	9.4×10
60	(7×10)	(6×10)

1 as described before. In this case equation (16) reduces to

$$\langle S^2 \rangle_U = l^2 \left\{ \frac{1}{3} \frac{1+2U}{1+U} + 1 - 2(1+U) \left[1 - \left(1 + \frac{U}{1+U} \right)^{-1/U} \right] \right\}. \quad (17)$$

The correction factor for crossover concentrations is therefore given by

$$\gamma(U=0.1) = \frac{(C_S^*)_{U=0}}{(C_S^*)_{U=0.1}} = \left[\frac{\langle S^2 \rangle_{U=0}}{\langle S^2 \rangle_{U=0.1}} \right]^{3/2} = 1.37. \quad (18)$$

From equations (12) and (14), a relation $N^* \sim C^{-1/2}$ is obtained, so that the correction factor for N^* becomes

$$\delta(U=0.1) = \frac{(N^*)_{U=0}}{(N^*)_{U=0.1}} = \left[\frac{(C_S^*)_{U=0}}{(C_S^*)_{U=0.1}} \right]^{-1/2} = 0.855. \quad (19)$$

The corrected crossover values are also listed in table II and plotted on the phase diagram in figure 1 with error bars. These values confirm C_S^* at least in a concentration range of 10^{-2} to 1 mol/l. The extrapolated crossovers, $C_S^* \approx 1.4$ and 3.8 mol/l for $\bar{M}_w = 2.2 \times 10^5$ and 1.2×10^6 , respectively, lie on the broken line for polyions with $b_t \approx l$, but this does not mean that in this very dilute concentration polyions have the b_t equal to l . This is only an evidence that polyions behave so in the concentrations used experimentally. If q_m 's could be measured in a very dilute range, C_S^* determined from them would be on the solid line for the rodlike chain model.

6. Discussion.

The dilute-semidilute crossover concentration for radius of gyration, C_S^* , has been confirmed in a concentration range between 10^{-2} to 1 mol/l by the SAXS technique. This crossover concentration is also confirmed by a dynamic method. Ito *et al.* [14] revealed that the high-frequency dielectric relaxation (MHz in order of magnitude) is caused by the fluctuation of loosely bound counterions in the direction normal to the polyion axis. The dielectric increment $\Delta\epsilon$ and the relaxation time τ are then related to the range of the fluctuation of counterions or the average distance between polyions [15]:

$$\Delta\epsilon \sim \begin{cases} \text{const} & (\text{semidilute}) \\ C^{1/3} N^{2/3} & (\text{dilute}) \end{cases} \quad (20)$$

and

$$\tau \sim \begin{cases} C^{-1} & (\text{semidilute}) \\ C^{-2/3} N^{2/3} & (\text{dilute}) \end{cases} \quad (21)$$

From the value of both $\Delta\epsilon$ and τ observed within the region of $2.4 \times 10^{-4} \text{ mol/l} \leq C \leq 2.9 \text{ mol/l}$ and $90 \leq N \leq 3,800$, they estimated the dilute-semidi-

lute crossover concentration C_ε^* by using equations (20) and (21) as

$$(C_\varepsilon^*/N)l^3 \approx 10, \quad (22)$$

which corresponds to $C_\varepsilon^* \approx 1.06 \times 10^3 N^{-2}$ in mol/l. The correction for polydispersity $\bar{M}_w/\bar{M}_n = 1.10$ of the used samples gives

$$C_\varepsilon^* \approx 1.45 \times 10^3 N^{-2} \text{ (mol/l)}. \quad (23)$$

This crossover concentration agrees surprisingly well to C_ξ^* for $\alpha = 1$ of equation (5).

We have some information on the melting concentration C_m^* though it is still preliminary. The distance distribution functions obtained from the SAXS curves by inverse Fourier transformation changes near C_m^* . The innermost correlation peak in this function deforms from a single peak to a peak with a shoulder or a doublet with decreasing concentration. This change is not due to a regular array of bound counterions because the substitution of sodium counterions by lithium ones gave almost the same distribution function. For lithium counterions with very less electrons, the newly appeared shoulder or subpeak would decrease greatly in intensity or disappear if the deformation were caused by the counterions. This deformation therefore seems to be

related to some regular structure of polyion, which is expected in the transition regime. Further, this change never occurs unless N is more than 90, which also supports the phase diagram since C_m^* ends at $N \approx 100$ and no transition regime exists for $N < 100$.

We have no noteworthy information on C_κ^* in the dilute region, but it would be checked by examining whether a single correlation peak appears. The SAXS intensity for a sample with $\bar{M}_w = 1.8 \times 10^3$ and $C = 5$ g/l was very weak, and it was buried in the background. Therefore we could not judge if there exists a correlation peak. As the neutron scattering provides a high contrast to polyions in heavy water, small-angle neutron scattering (SANS) would make possible such a judgement. The experiments to evidence the second lattice regime in high C and low N are being made by using SAXS.

Acknowledgments.

We wish to thank Professor R. Koyama of College of General Education, Kyoto University for useful discussions, especially on his theory. One of the authors (K. K.) would like to express his sincere thanks to Professor P. G. de Gennes of College de France for the interest in this study and the useful comments.

References

- [1] KAJI, K., URAKAWA, H., KANAYA, T., KITAMARU, R., *Macromolecules* **17** (1984) 1835.
- [2] DE GENNES, P. G., PINCUS, P., VELASCA, R. M., BROCHARD, F., *J. Phys. France* **37** (1976) 1461.
- [3] ODIJK, T., *Macromolecules* **12** (1979) 688.
- [4] LE BRET, M., *J. Chem. Phys.* **76** (1982) 6243.
- [5] NIERLICH, M., BOUE, F., LAPP, A., OBERTHUR, R., *Colloid Polym. Sci.* **263** (1985) 955.
- [6] MANDEL, M., *Eur. Polym. J.* **19** (1983) 911.
- [7] KOYAMA, R., *Macromolecules* **17** (1984) 1594.
KOYAMA, R., *Macromolecules* **19** (1985) 178.
- [8] DE GENNES, P. G., Private Communication to K. Kaji.
- [9] YAMAKAWA, H., *Modern Theory of Polymer Solutions* (Harper & Row Pub., New York) 1971.
- [10] HIRAGI, Y., URAKAWA, H., TANABE, K., *J. Appl. Phys.* **58** (1985) 5.
- [11] NIERLICH, M., WILLIAMS, C. E., BOUE, F., COTTON, J. P., DAOU, M., FARNOUX, B., JANNINK, G., PICOT, C., MOAN, M., WOLFF, C., RINAUDO, M., DE GENNES, P. G., *J. Phys. France* **40** (1979) 701.
- [12] HAYTER, J., JANNINK, G., BROCHARD-WYART, F., DE GENNES, P. G., *J. Phys. Lett. France* **41** (1980) L-451.
- [13] OBERTHÜR, R. C., *Makromol. Chem.* **179** (1978) 2693.
- [14] ITO, K., OOKUBO, N., HAYAKAWA, R., *Rep. Prog. Polym. Phys. Jpn* **29** (1986) 83.
- [15] ITO, K., YAGI, A., OOKUBO, N., HAYAKAWA, R., *Rep. Prog. Polym. Phys. Jpn* **29** (1986) 87.
- [16] JANNINK, G., *Makromol. Chem. Macromol. Symp.* **1** (1986) 67.
- [17] WEILL, G., MARET, G., ODIJK, T., *Polymer* **25** (1984) 147.
- [18] ODIJK, T., HOUWAART, A. C., *J. Polym. Sci. Polym. Phys. Ed.* **16** (1978) 627.